J Mol Model (2013) 19:4849–4856
DOI 10.1007/s00894-013-1987-5

ORIGINAL PAPER

A comparative DFT study on aquation and nucleobase binding of ruthenium (II) and osmium (II) arene complexes

Hanlu Wang · Xingye Zeng · Rujin Zhou · Cunyuan Zhao

Received: 16 July 2013 / Accepted: 27 August 2013 / Published online: 15 September 2013

Abstract The potential energy surfaces of the reactions of organometallic arene complexes of the type [(η^6-arene)M^{II}(pic)Cl] (where pic = 2-picolinic acid, M = Ru or Os) were examined by a DFT computational study. Among the seven density functional methods, hybrid exchange functional B3LYP outperforms the others to explain the aquation of the complexes. The reactions and binding energies of Ru^{II} and Os^{II} arene complexes with both 9EtG and 9EtA were studied to gain insight into the reactivity of these types of organometallic complexes with DNA. The obtained data rationalize experimental observation, contributing to partly understanding the potential biological and medical applications of organometallic complexes.

Keywords DFT · Ruthenium · Osmium · Aquation · Nucleobase

Electronic supplementary material The online version of this article (doi:10.1007/s00894-013-1987-5) contains supplementary material, which is available to authorized users.

H. Wang (✉)
College of Chemistry and Life Science, Guangdong University of Petrochemical Technology, Maoming 525000, People's Republic of China
e-mail: wanghlu@mail2.sysu.edu.cn

X. Zeng · R. Zhou
College of Chemical and Environmental Engineering, Guangdong University of Petrochemical Technology, Maoming 525000, People's Republic of China

C. Zhao
MOE Key Laboratory of Bioinorganic and Synthetic Chemistry/KLGHEI of Environment and Energy Chemistry, School of Chemistry and Chemical Engineering, Sun Yat-Sen University, Guangzhou 510275, People's Republic of China

Introduction

It is well known that platinum anticancer drugs are in routine clinical use and under clinical development worldwide [1]. With the sharp rise in global cancer incidence and mortality, the development of new effective anticancer drugs has been a major focus in this field. Ruthenium complexes are one of the most promising non-platinum anticancer drugs [2–18]. Although osmium (a third row transitional metal) complexes have a reputation for being either toxic (OsO_4) or substitution-inert, the chemical and biological activity of half-sandwich osmium arene complexes is currently becoming an active area of research [19–33]. Ruthenium and osmium arene complexes [(η^6-arene)M(XY)Z]$^{n+}$ (XY = bidentate ligand) were reported to exhibit anticancer activity comparable to that of the clinical drugs carboplatin and cisplatin [2–33].

A number of theoretical works have focused on the anticancer ruthenium and osmium arene complexes. Wang et al. [34] investigated the aquation processes (substitution of X by H_2O) of Ru^{II} arene complexes using the DFT (PW91) method. Dorcier et al. [35] discussed the binding energies between the metal (Ru and Os) centers and the surrounding ligands with DFT, and the results were in accordance with data obtained using electrospray ionization mass spectrometry. An investigation on the structural and energetic properties of [(η^6-arene)Ru^{II}(en)Cl]$^+$ (en = ethylenediamine) anticancer compounds and their interaction with nucleobases using DFT (BP86) and MP2 calculations together with Car-Parrinello molecular dynamics has been reported by Rothlisberger and coworkers [36, 37]. They also studied the binding processes of two Ru^{II} arene complexes to double-stranded DNA using classical and QM/MM molecular dynamics simulations [38]. Gkionis and coworkers [39] explored the DNA binding of ruthenium arene complexes and represented the role of hydrogen bonding and π stacking. The structure, stability and

reactivity of $[(\eta^6\text{-arene})Ru^{II}(en)Cl]^+$ were further characterized by Burda [40, 41] using several theoretical methods. More recently, we have also reported a series work on the relationships between the structures and anticancer activities for Ru and Os arene complexes [42–44].

Organometallic arene complexes of the type $[(\eta^6\text{-arene})M^{II}(pic)Cl]$ (where pic = 2-picolinic acid, M = Ru or Os) offer much potential for exploration as anticancer agents due to the large diversity of structure and bonding modes [15, 18, 23, 25–27, 29]. We have discussed in detail the aquation mechanism of $[(\eta^6\text{-}p\text{-cym})M^{II}(pic)Cl]$ (where M = Ru or Os) in our previous work, in which the effect of arene ligand and the nucleobase substitution were not discussed for reasons of space [43]. DNA is a potential biological target for classical transition-metal anticancer drugs, suggesting that it is important to clarify the reaction mechanism of nucleobase substitution. In the present study, we explored the influence of the metal center and arene on aquation and the interactions with nucleobases of a series of picolinate complexes. The first part of the present study discusses the similarities and differences in the aquation of Ru^{II} and Os^{II} complexes. We then examine the subsequent nucleobase substitution of the Ru and Os complexes, which could provide the access to transition structures and predict the trends in the reactivity and selectivity of these complexes toward biological targets.

Computational methods

The general structure of this class of complexes is drawn in Fig. 1, where a pseudo octahedral arrangement of the Os and Ru is assumed. The compounds of $[(\eta^6\text{-arene})M^{II}(pic)Cl]$, ($\eta^6$-arene = benzene (bz), *p*-cymene (cym), biphenyl (bip), M = Ru and Os, pic = 2-picolinic acid) were examined using DFT methods with B3LYP hybrid functional [45, 46]. The 6-31G** basis sets were employed for H-, C-, N-, O- and Cl-atoms, and the LanL2DZ basis set was employed for Os and Ru [47–49], labeled as BS1. Geometry optimizations were then redone using the COSMO implicit solvent approach with dielectric constant $\varepsilon = 78.36$ [50, 51]. Thermal energies were extracted from vibrational frequency calculations, which were used to verify the correct nature of the stationary points at 298.15 K and 1 atm. The frequency calculations also served for confirmation of the correct character of transition state (TS) structures as well as reactant and product (super) molecules. To obtain accurate energies for the reaction surfaces, single-point energies were further calculated based on the ground state structures using a higher basis set of LanL2DZ-(f) used for Ru and Os ($\zeta_f = 1.235$ for Ru and $\xi_f = 0.886$ for Os) [52] and 6-311++G** for all other atoms, labeled as BS2.

The reported binding energies (BEs) were calculated using the general formulas

$$E_{binding} = E\left(M^{II}XY\right) + E(Z) - E\left(M^{II}XYZ\right) \quad (1)$$

whereM = Ru, Os, X = arene, Y = pic, and Z = 9EtG, 9EtA.

As Fig. 2 describes, the first reaction profile considered was the substitution of chloride by water, namely, aquation; the second reaction profile was the replacement of the aqua-ligand with model nucleobases [9-ethyl guanine (9EtG) and 9-ethyl adenine (9EtA)], since they are the most preferred nucleotide binding sites for many transition metal ions. All geometry optimization and single-point calculations were carried out using the Gaussian 09 program [53].

Results and discussion

For readability, acronyms are adopted throughout instead of the full chemical formulas. Definitions of abbreviations used are reported in the Appendix.

Hydrolysis processes

Generally, the chloride ligand acts as a leaving group during the aquation of the complexes, giving access to a coordination site that can be used to form an M–O bond

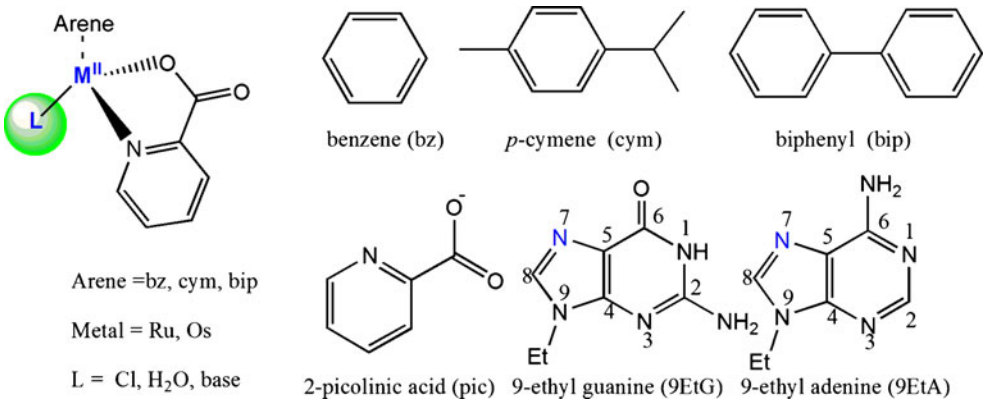

Fig. 1 Structures of the Os^{II} and Ru^{II} arene complexes

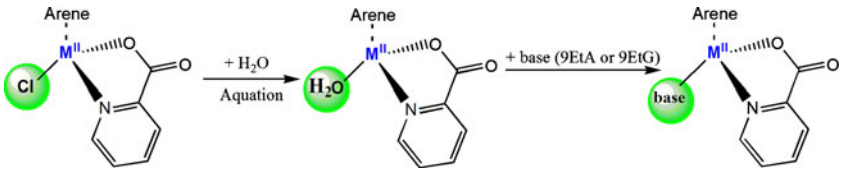

Fig. 2 Reactions of [(η^6-arene)M^{II}(pic)Cl] (M = Ru and Os)

to the water molecule. The aqua species are often more reactive than the relevant chloride complexes, and these Ru^{II} and Os^{II} arene anticancer complexes were activated via the same mechanism as cisplatin and their analogues [19, 20, 34, 54]. The aquation mechanism of the arene complexes studied can be generalized as shown in Fig. 3. A previous study performed by Wang et al. [43] demonstrated that the water molecule could be attacking in three orientations, and that water attacking in the back was unfavorable and ascribed to a large conformational change. Therefore, we considered only the most favorable "model A" as mentioned in reference [43]. These reactions belong to the class of second-order nucleophilic substitution (S_N2) reactions and the rate-limiting step is from the first intermediate (IM1) toward the second intermediate (IM2) via the transition state (step IM1→IM2).

Many DFT methods have been used to report the reaction of transitional metal arene complexes. One of the most popular methods is B3LYP. In this work, we carefully chose an appropriate set of exchange and correlation functionals when using DFT methods. Table 1 shows the activation free energies (ΔG_a) for the hydrolysis processes (Fig. 1) obtained with different computational methods, B97-D [55], CAM-B3LYP [56], BHandHLYP [57], BP86, M06L [58], B3PW91 [45, 59]. It was found that B97-D overestimated ΔG_a significantly, and M06L underestimated ΔG_a significantly (see Table 1). Among these methods, only M06L and B3LYP predicted the correct aquation trend for the osmium complexes compared to experimental values (cym-Os < bz-Os < bip-Os). Moreover, the results of B3LYP are closer to experimental measurements [23, 25, 27]. Consequently, the B3LYP method was adopted in the following computational study. The corresponding important parameter bond lengths and angles for optimized geometries for the aquation of six complexes are shown in Fig. 3. All reactant and product complexes exhibit "pseudooctahedral coordination" around the central metal atom, and the water molecules form hydrogen bonds with the negative chlorides or pic group. Inspection of the geometries of the transition states, the vibrational modes of the transition states (TS_{aqua}) present an angular vibrational mode between the leaving chloride and the incoming water. The optimized transition structures of Os are slightly more compact than those of Ru, due to the lanthanide contraction of Os [42].

Compared with experimental values determined by UV–vis spectrometry [23, 25, 27], the calculated results overestimated the measured rate constants by about two orders as reported in Table 1 [23, 25, 27]. The hydrolysis process is significantly more favorable for Ru^{II} complexes than for Os^{II} complexes, which is in agreement with the experimental observations [23, 25, 27]. Thus, the Ru^{II} arene complexes may hydrolyze too fast to be deactivated before reaching the target sites. As illustrated in Table 1, free energies of activation are both in the trend of cym-M < bz-M < bip-M for Ru^{II} and Os^{II} complexes. There is little difference between these values, indicating that the character of the arene ligand influences the reactivity of this type of complex to only a limited extent.

Interactions with nucleobase 9EtG and 9EtA

As DNA is a potential biological target for classical transition-metal anticancer drugs, reactions of Ru^{II} and Os^{II} arene complexes with nucleobases are of great importance. The nucleobase substitution of Ru arene complexes with en has been intensively studied theoretically at a wide range of different levels of theory [37–40, 60]. Differently, metal

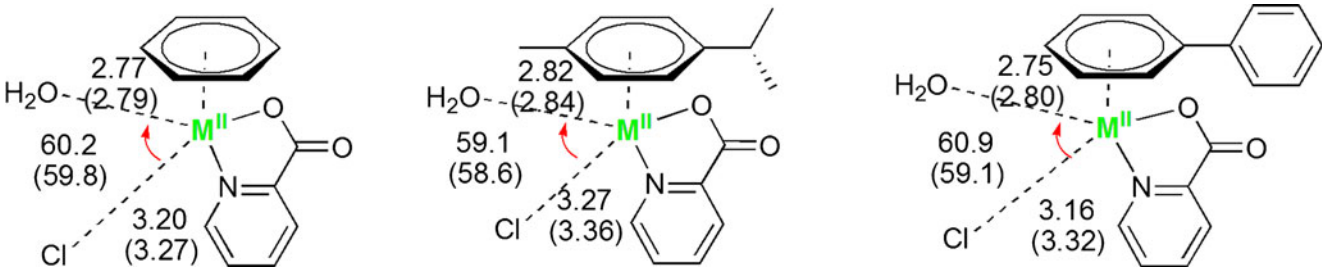

Fig. 3 Optimized geometric parameters bond lengths (Å) and angles (°) for transition states in the aquation of Os (Ru) complexes (M = Ru, Os; values in *brackets* are for Ru)

Table 1 ΔG_a (kcal/mol^{-1}) and r (s^{-1}) of the aquation with different computational methods

	bz-Ru	cym-Ru	bip-Ru	bz-Os	cym-Os	bip-Os
B97-D	25.8	27.0	27.4			
CAM-B3LYP	19.2	17.8	18.2	22.7	21.5	21.7
BHandHLYP	18.9	17.5	16.0	22.0	21.1	21.3
BP86	17.9	17.0	17.0	21.1	20.3	20.8
M06L	13.4	13.1	13.5	16.8	16.0	17.5
B3PW91	19.4	18.5	18.3	23.2	24.2	22.9
B3LYP	17.5	16.5	16.0	21.4	21.0	22.4
r (B3LYP)				1.30E-03	2.5E-03	2.40E-04
r (exptl) [23]				4.5E-04	5.0E-04	2.0E-04

arene complexes with en prefer 9EtG to 9EtA [19, 20, 61], whereas complexes with pic ligand bind to both 9EtG and 9EtA [23]. The ruthenium complexes are well-known to undergo associative ligand substitution reactions via a pseudo seven-coordinated transition state [40, 60]. Thus, it is necessary to include the water ligand for a realistic simulation of the kinetics of bond formation between metal and nucleobase, as displayed in Fig. 4. To gain insight into the reactivity of these types of organometallic complexes with DNA, we studied the reaction of Ru^{II} and Os^{II} arene complexes with model 9EtG and 9EtA (arene = bz).

The [M-H_2O + 9EtG (9EtA)] as a reference state is adopted to compute the activation barriers. For the sake of calculation efficiency, only 9EtG and 9EtA cis to aqua ligand reactions were considered, as the trans to aqua was demonstrated to be unfavorable [37].

These reactions are of the nucleobase-water exchange reaction type, and the transition states correspond to the breaking of the M–O(wat) bond and the forming of the M-N7(nucleobase) bond, as shown in Fig. 4. The reaction energy profile for the nucleobase substitution mechanisms is presented in Fig. 5. The reaction of 9EtG with bz-Ru should overcome a 26.1 kcal/mol^{-1} activation energy and that of bz-Os is a little higher, being 28.2 kcal/mol^{-1}. As for the reactions of 9EtA, the free energies of activation for bz-Ru and bz-Os are close, being 25.2 and 25.4 kcal/mol^{-1}, respectively. The above results show that the reaction of 9EtA is slightly more favorable than that of 9EtG for both Ru and Os arene complexes. Figure 5 shows that the formation of bz-Ru-G and bz-Os-G are exothermic by 0.5 and 3.5 kcal/mol^{-1}, respectively. In contrast, the formation of bz-Ru-A is endothermic by 2.2 kcal/mol^{-1}, and that of bz-Ru-A is exothermic by 2.0 kcal/mol^{-1}. The more exothermic values for 9EtG complexes formation indicate that 9EtG is the thermodynamically more stable product. Hence, once guanine adducts (on DNA or RNA) are formed, they are likely to persist. Experimental observations show that the binding constant of 9EtA is moderate (log$K$=3.95), and the equilibrium for dissociation of 9EtA from [(η^6-p-cym)Os^{II}(pic)(9EtA-N7)]$^+$ is reached within 24 h of incubation (310 K). However, the dissociation of 9EtG from [(η^6-p-cym)Os^{II}(pic)(9EtG-N7)]$^+$ occurs slowly (equilibrium is not reached even after incubation at 310 K for 13 days) [23].

Hydrogen bonding is an important factor in the preference of the complexes for 9EtA substitution. The transition structures of 9EtA substitution exhibit two strong H-bonds: (A)N7···H–O(water) and (N6)H···O1 (pic) (see Fig. 4), and these strong H-bonds may play an important role in the biological activity, since DNA is a potential target site for these complexes [2, 3, 36, 37, 62, 63]. On the other hand, the size of the lone-pair lobe at the N7 position is larger for 9EtG than 9EtA as demonstrated by Lippard [64], indicative of a larger interaction between 9EtG

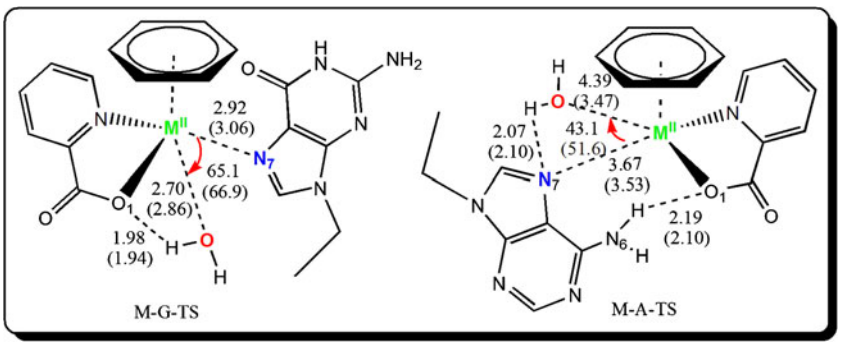

Fig. 4 Optimized geometric parameters bond lengths (Å) and angles (°) for transition states in the nucleobase substitution (M = Ru and Os, and values in *brackets* are for Ru)

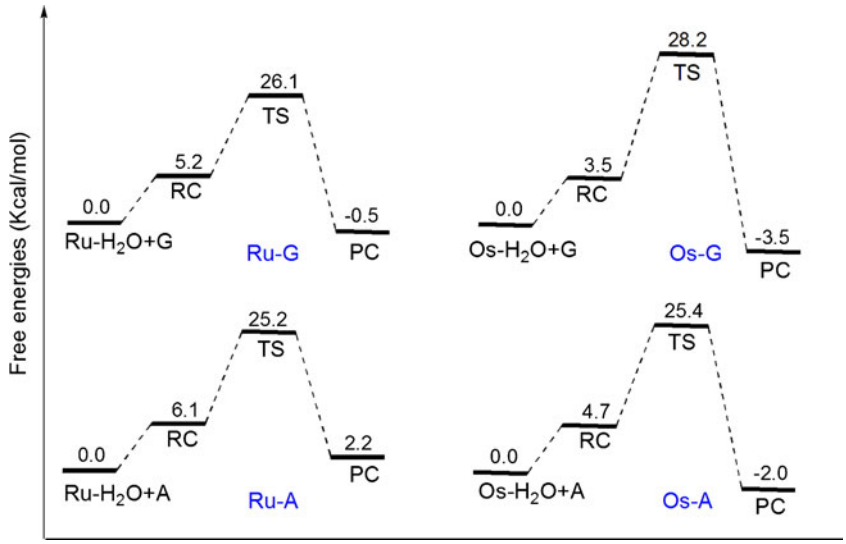

Fig. 5 Free energy (kcal/mol^{-1}) profiles of nucleobase substitution of complexes in aqueous phase at B3LYP/BS2// B3LYP/BS1

and the metal center. These two antagonistic effects result in good affinity to both 9EtG and 9EtA for pic complexes, which is in good agreement with experimental observations [23].

Binding energies for nucleobases

The binding energies were calculated according to Eq. 1 in the COSMO approach, and are collected in Table 2. Comparison of binding energies for model 9EtG and 9EtA complexes is important, since the nucleophilic sites of these bases are available for complexation in duplex DNA and are therefore the primary sites of metalation. The former are found to be only slightly stable by approximately 1 kcal/mol^{-1}, except the arene ligand is cym in which the 9EtG and 9EtA binding energies are almost equivalent. These data are again in agreement with experiments, which indicate a preference for binding to G over A bases for pic complexes [23]. The equivalent comparison for $[(\eta^6\text{-arene})Ru^{II}(en)]^{2+}$ complexes has been calculated previously at ca. 5 kcal/mol^{-1} in aqueous solution [39]. The above analysis indicates that the pic complexes show lower selectivity for G and A than for en complexes. The nucleobase binding for both Ru and Os complexes followed the trend: bz > bip > cym, which could be due mainly to the steric effect of the arene ligand.

Conclusions

A series of potential anticancer Ru^{II} and Os^{II} pic complexes with different arene ligands was investigated using several DFT methods; B3LYP was demonstrated to be the best among them. The aquation proceeded through S_N2 reaction mechanism. The reaction barriers and rates were obtained for aquation of the complexes, and it was revealed that the rate of aquation was very slow for Os^{II} complexes although their structures are similar to those of Ru^{II} complexes. This partly explains the inactivity of the osmium arene complexes. In addition, the character of the arene ligand slightly influenced the aquation rate of this type of complexes.

The reaction mechanisms of Os^{II} and Ru^{II} arene pic complexes with 9EtG and 9EtA were explored in detail. Both of the 9EtA and 9EtG substitution proceeded in concerted steps with dissociative characteristics. The activation barriers of the reaction of Os^{II} complexes with 9EtA and 9EtG are higher than those of Ru^{II}. Additionally, Ru and Os adducts of 9EtG are more stable than those of 9EtA, which is in agreement with experimental observations. The obtained binding energies also verified this reality. This could be ascribed to two antagonistic effects: H-bonds between 9EtA and pic, and the stronger interaction between 9EtG and the metal center. The above results might contribute to understanding the observed contrasting biological properties for Ru^{II} and Os^{II} arene complexes.

Table 2 Binding energies (kcal/mol^{-1}) of the nucleobases at B3LYP/BS2// B3LYP/BS1

	cym-Ru-G	bz-Ru-G	bip-Ru-G	cym-Os-G	bz-Os-G	bip-Os-G
E	21.5	25.1	23.1	22.5	26.2	24.8
	cym-Ru-A	bz-Ru-A	bip-Ru-A	cym-Os-A	bz-Os-A	bip-Os-A
E	21.6	24.6	22.4	22.9	25.3	23.6

Acknowledgments This work was supported by the National Natural Science Foundation of China (Nos., 21173273) and Dr. Start Fund of Guangdong University of Petrochemical Technology.

Appendix

Abbreviations

Acronym	Chemical Formula
pic	2-picolinic acid
p-cym	*p*-cymene
bip	biphenyl
bz	benzene
9EtG	9-ethyl guanine
9EtA	9-ethyl adenine
Ru-H_2O	$[(\eta^6\text{-bz})Ru^{II}(pic)(H_2O)]^{2+}$
bz-Ru-A	$[(\eta^6\text{-bz})Ru^{II}(pic)(9EtA)]^{2+}$
bz-Os-A	$[(\eta^6\text{-bz})Os^{II}(pic)(9EtA)]^{2+}$
cym-Ru	$[(\eta^6\text{-}p\text{-cym})Ru^{II}(pic)Cl]^{+}$
cym-Os	$[(\eta^6\text{-}p\text{-cym})Os^{II}(pic)Cl]^{+}$
bip-Ru	$[(\eta^6\text{-bip})Ru^{II}(pic)Cl]^{+}$
bip-Os	$[(\eta^6\text{-bip})Os^{II}(pic)Cl]^{+}$
bz-Ru	$[(\eta^6\text{-bz})Ru^{II}(pic)Cl]^{+}$
bz-Os	$[(\eta^6\text{-bz})Os^{II}(pic)Cl]^{+}$
Os-H_2O	$[(\eta^6\text{-bz})Os^{II}(pic)(H_2O)]^{2+}$
bz-Ru-G	$[(\eta^6\text{-bz})Ru^{II}(pic)(9EtG)]^{2+}$
bz-Os-G	$[(\eta^6\text{-bz})Os^{II}(pic)(9EtG)]^{2+}$

References

1. Reedijk J (2009) Platinum anticancer coordination compounds: study of DNA binding inspires new drug design. Eur J Inorg Chem 2009:1303–1312
2. Liu HK, Berners-Price SJ, Wang FY, Parkinson JA, Xu JJ, Bella J, Sadler PJ (2006) Diversity in guanine-selective DNA binding modes for an organometallic ruthenium arene complex. Angew Chem Int Ed 45:8153–8156
3. Liu HK, Wang FY, Parkinson JA, Bella J, Sadler PJ (2006) Ruthenation of duplex and single-stranded d(CGGCCG) by organometallic anticancer complexes. Chem Eur J 12:6151–6165
4. Dyson PJ (2007) Systematic design of a targeted organometallic antitumor drug in pre-clinical development. Chimia 61:698–703
5. Sadler PJ, Peacock AFA (2008) Medicinal organometallic chemistry: designing metal arene complexes as anticancer agents. Chem Asian J 3:1890–1899
6. Schuecker R, John RO, Jakupec MA, Arion VB, Keppler BK (2008) Water-soluble mixed-ligand ruthenium(II) and osmium(II) arene complexes with high antiproliferative activity. Organometallics 27:6587–6595
7. van Rijt SH, Sadler PJ (2009) Current applications and future potential for bioinorganic chemistry in the development of anticancer drugs. Drug Discov Today 14:1089–1097
8. Levina A, Mitra A, Lay PA (2009) Recent developments in ruthenium anticancer drugs. Metallomics 1:458–470
9. Pizarro AM, Sadler PJ (2009) Unusual DNA binding modes for metal anticancer complexes. Biochimie 91:1198–1211
10. Grguric-Sipka S, Stepanenko IN, Lazic JM, Bartel C, Jakupec MA, Arion VB, Keppler BK (2009) Synthesis, X-ray diffraction structure, spectroscopic properties and antiproliferative activity of a novel ruthenium complex with constitutional similarity to cisplatin. Dalton Trans 38:3334–3339
11. Suss-Fink G (2010) Arene ruthenium complexes as anticancer agents. Dalton Trans 39:1673–1688
12. Hanif M, Nazarov AA, Hartinger CG, Kandioller W, Jakupec MA, Arion VB, Dyson PJ, Keppler BK (2010) Osmium(II)–versus ruthenium(II)–arene carbohydrate-based anticancer compounds: similarities and differences. Dalton Trans 39:7345–7352
13. Arndt M, Salih KSM, Fromm A, Goossen LJ, Menges F, Niedner-Schatteburg G (2011) Mechanistic investigation of the Ru-catalyzed hydroamidation of terminal alkynes. J Am Chem Soc 133:7428–7449
14. Arion VB, Dobrov A, Göschl S, Jakupec MA, Keppler BK, Rapta P (2012) Ruthenium- and osmium-arene-based paullones bearing a TEMPO free-radical unit as potential anticancer drugs. Chem Commun 48:8559–8561
15. Gligorijević N, Aranđelović S, Filipović L, Jakovljević K, Janković R, Grgurić-Šipka S, Ivanović I, Radulović S, Tešić ŽL (2012) Picolinate ruthenium(II)–arene complex with in vitro antiproliferative and antimetastatic properties: comparison to a series of ruthenium(II)–arene complexes with similar structure. J Inorg Biochem 108:53–61
16. Kurzwernhart A, Kandioller W, Bächler S, Bartel C, Martic S, Buczkowska M, Mühlgassner G, Jakupec MA, Kraatz H-B, Bednarski PJ et al (2012) Structure–activity relationships of targeted $Ru^{II}(\eta^6\text{-}p\text{-cymene})$ anticancer complexes with flavonol-derived ligands. J Med Chem 55:10512–10522
17. Wu K, Luo Q, Hu W, Li X, Wang F, Xiong S, Sadler PJ (2012) Mechanism of interstrand migration of organoruthenium anticancer complexes within a DNA duplex. Metallomics 4:139–148
18. Habtemariam A, Melchart M, Fernandez R, Parsons S, Oswald ID, Parkin A, Fabbiani FP, Davidson JE, Dawson A, Aird RE et al (2006) Structure-activity relationships for cytotoxic ruthenium(II) arene complexes containing N, N-, N, O-, and O, O-chelating ligands. J Med Chem 49:6858–6868
19. Peacock AFA, Habtemariam A, Fernandez R, Walland V, Fabbiani FPA, Parsons S, Aird RE, Jodrell DI, Sadler PJ (2006) Tuning the reactivity of osmium(II) and ruthenium(II) arene complexes under physiological conditions. J Am Chem Soc 128:1739–1748
20. Peacock AFA, Habtemariam A, Moggach SA, Prescimone A, Parsons S, Sadler PJ (2007) Chloro half-sandwich osmium(II) complexes: influence of chelated N, N-ligands on hydrolysis, guanine binding, and cytotoxicity. Inorg Chem 46:4049–4059
21. Peacock AFA, Melchart M, Deeth RJ, Habtemariam A, Parsons S, Sadler PJ (2007) Osmium(II) and ruthenium(II) arene maltolato complexes: rapid hydrolysis and nucleobase binding. Chem Eur J 13:2601–2613
22. Arion VB, Schmid WF, John RO, Jakupec MA, Keppler BK (2007) Highly antiproliferative ruthenium(II) and osmium(II) arene complexes with paullone-derived ligands. Organometallics 26:6643–6652
23. Peacock AFA, Parsons S, Sadler PJ (2007) Tuning the hydrolytic aqueous chemistry of osmium arene complexes with N, O-chelating ligands to achieve cancer cell cytotoxicity. J Am Chem Soc 129:3348–3357
24. Kostrhunova H, Florian J, Novakova O, Peacock AFA, Sadler PJ, Brabec V (2008) DNA interactions of monofunctional organometallic osmium(II) antitumor complexes in cell-free media. J Med Chem 51:3635–3643
25. van Rijt SH, Peacock AFA, Johnstone RDL, Parsons S, Sadler PJ (2009) Organometallic osmium(II) arene anticancer complexes containing picolinate derivatives. Inorg Chem 48:1753–1762

26. van Rijt SH, Hebden AJ, Amaresekera T, Deeth RJ, Clarkson GJ, Parsons S, McGowan PC, Sadler PJ (2009) Amide linkage isomerism as an activity switch for organometallic osmium and ruthenium anticancer complexes. J Med Chem 52:7753–7764
27. van Rijt SH, Mukherjee A, Pizarro AM, Sadler PJ (2010) Cytotoxicity, hydrophobicity, uptake, and distribution of osmium(II) anticancer complexes in ovarian cancer cells. J Med Chem 53:840–849
28. Filak LK, Muhlgassner G, Bacher F, Roller A, Galanski M, Jakupec MA, Keppler BK, Arion VB (2011) Ruthenium- and osmium-arene complexes of 2-substituted indolo[3,2-c]quinolines: synthesis, structure, spectroscopic properties, and antiproliferative activity. Organometallics 30:273–283
29. van Rijt SH, Kostrhunova H, Brabec V, Sadler PJ (2011) Functionalization of osmium arene anticancer complexes with (poly)arginine: effect on cellular uptake, internalization, and cytotoxicity. Bioconjug Chem 22:218–226
30. Fu Y, Romero MJ, Habtemariam A, Snowden ME, Song L, Clarkson GJ, Qamar B, Pizarro AM, Unwin PR, Sadler PJ (2012) The contrasting chemical reactivity of potent isoelectronic iminopyridine and azopyridine osmium(ii) arene anticancer complexes. Chem Sci 3:2485
31. Henkea H, Kandiollera W, Hanifc M, Kepplera BK, Hartinger CG (2012) Organometallic ruthenium and osmium compounds of pyridin-2- and -4-ones as potential anticancer agents. Chem Biodivers 9:1718–1727
32. Filak LK, Göschl S, Heffeter P, Ghannadzadeh Samper K, Egger AE, Jakupec MA, Keppler BK, Berger W, Arion VB (2013) Metal–arene complexes with indolo[3,2-c]-quinolines: effects of ruthenium vs osmium and modifications of the lactam unit on intermolecular interactions, anticancer activity, cell cycle, and cellular accumulation. Organometallics 32:903–914
33. Romero-Canelón I, Salassa L, Sadler PJ (2013) The contrasting activity of iodido versus chlorido ruthenium and osmium arene azo- and imino-pyridine anticancer complexes: control of cell selectivity, cross-resistance, p53 dependence, and apoptosis pathway. J Med Chem 56:1291–1300
34. Wang FY, Habtemariam A, van der Geer EPL, Fernandez R, Melchart M, Deeth RJ, Aird R, Guichard S, Fabbiani FPA, Lozano-Casal P et al (2005) Controlling ligand substitution reactions of organometallic complexes: tuning cancer cell cytotoxicity. Proc Natl Acad Sci USA 102:18269–18274
35. Dorcier A, Dyson PJ, Gossens C, Rothlisberger U, Scopelliti R, Tavernelli I (2005) Binding of organometallic ruthenium(II) and osmium(II) complexes to an oligonucleotide: a combined mass spectrometric and theoretical study. Organometallics 24:2114–2123
36. Gossens C, Tavernelli I, Rothlisberger U (2007) Structural and energetic properties of organometallic ruthenium(II) diamine anticancer compounds and their interaction with nucleobases. J Chem Theory Comput 3:1212–1222
37. Gossens C, Tavernelli I, Rothlisberger U (2009) Binding of organometallic ruthenium(II) anticancer compounds to nucleobases: a computational study. J Phys Chem A 113:11888–11897
38. Gossens C, Tavernelli I, Rothlisberger U (2008) DNA structural distortions induced by ruthenium-arene anticancer compounds. J Am Chem Soc 130:10921–10928
39. Gkionis K, Platts JA, Hill JG (2008) Insights into DNA binding of ruthenium arene complexes: role of hydrogen bonding and pi stacking. Inorg Chem 47:3893–3902
40. Futera Z, Klenko J, Sponer JE, Sponer J, Burda JV (2009) Interactions of the "piano-stool" [ruthenium(II)(η^6-arene)(en)Cl]$^+$ complexes with water and nucleobases; ab initio and DFT study. J Comput Chem 30:1758–1770
41. Chval Z, Futera Z, Burda JV (2011) Comparison of hydration reactions for "piano-stool" RAPTA-B and [Ru(η^6-arene)(en)Cl]$^+$ complexes: density functional theory computational study. J Chem Phys 134:024520
42. Wang HL, DeYonker NJ, Gao H, Ji LN, Zhao CY, Mao Z-W (2012) Mechanism of aquation and nucleobase binding of ruthenium (II) and osmium (II) arene complexes: a systematic comparison DFT study. J Organomet Chem 704:17–28
43. Wang HL, DeYonker NJ, Gao H, Tan CP, Zhang XT, Ji LN, Zhao CY, Mao Z-W (2012) Aquation and dimerization of osmium(II) anticancer complexes: a density functional theory study. RSC Adv 2:436–446
44. Wang HL, DeYonker NJ, Zhang XT, Zhao CY, Ji LN, Mao Z-W (2012) Photodissociation of a ruthenium(II) arene complex and its subsequent interactions with biomolecules: a density functional theory study. J Mol Model 18:4675–4686
45. Lee C, Yang W, Parr RG (1988) Development of the Colle-Salvetti conelation energy formula into a functional of the electron density. Phys Rev B 37:785–789
46. Becke AD (1993) Density-functional thermochemistry. III. The role of exact exchange. J Chem Phys 98:5648–5652
47. Wadt WR, Hay PJ (1985) Ab initio effective core potentials for molecular calculations. Potentials for main group elements Na to Bi. J Chem Phys 82:284–298
48. Hay PJ, Wadt WR (1985) Ab initio effective core potentials for molecular calculations. Potentials for K to Au including the outermost core orbitals. J Chem Phys 82:299–310
49. Hay PJ, Wadt WR (1985) Ab initio effective core potentials for molecular calculations. Potentials for the transition metal atoms Sc to Hg. J Chem Phys 82:270–283
50. Klamt A (1995) Conductor-like screening model for real solvents: a new approach to the quantitative calculation of solvation phenomena. J Phys Chem 99:2224–2235
51. Klamt A, Schüürmann G (1993) COSMO: a new approach to dielectric screening in solvents with explicit expressions for the screening energy and its gradient. J Chem Soc Perkin Trans 2: 799–805
52. Ehlers W, Böhme M, Dapprich S, Gobbi A, Höllwarth A, Jonas V, Köhler KF, Stegmann R, Veldkamp A, Frenking G (1993) A set of f-polarization functions for pseudo-potential basis sets of the transition metals Sc-Cu, Y-Ag and La-Au. Chem Phys Lett 208: 111–114
53. Frisch MJ et al (2010) Gaussian 09, revision A.01. Gaussian, Wallingford
54. Wang F, Chen HM, Parsons S, Oswald LDH, Davidson JE, Sadler PJ (2003) Kinetics of aquation and anation of ruthenium(II) arene anticancer complexes, acidity and X-ray structures of aqua adducts. Chem Eur J 9:5810–5820
55. Grimme S (2006) Semiempirical GGA-type density functional constructed with a long-range dispersion correction. J Comput Chem 27:1787–1799
56. Yanai T, Tew DP, Handy NC (2004) A new hybrid exchange-correlation functional using the Coulomb-attenuating method (CAM-B3LYP). Chem Phys Lett 393:51–57
57. Becke AD (1993) A new mixing of Hartree-Fock and local density-functional theories. J Chem Phys 98:1372–1377
58. Zhao Y, Truhlar DG (2008) The M06 suite of density functionals for main group thermochemistry, thermochemical kinetics, noncovalent interactions, excited states, and transition elements: two new functionals and systematic testing of four M06-class functionals and 12 other functionals. Theor Chem Accounts 120: 215–241
59. Stephens PJ, Devlin FJ, Chabalowski CF, Frisch MJJ (1994) Ab initio calculation of vibrational absorption and circular dichroism spectra using density functional force fields. Phys Chem 98: 11623–11627
60. Deubel DV, Lau JKC (2006) In silico evolution of substrate selectivity: comparison of organometallic ruthenium complexes with the anticancer drug cisplatin. Chem Commun 2006:2451–2453

61. Chen HM, Parkinson JA, Morris RE, Sadler PJ (2003) Highly selective binding of organometallic ruthenium ethylenediamine complexes to nucleic acids: novel recognition mechanisms. J Am Chem Soc 125:173–186
62. Chen HM, Parkinson JA, Novakova O, Bella J, Wang FY, Dawson A, Gould R, Parsons S, Brabec V, Sadler PJ (2003) Induced-fit recognition of DNA by organometallic complexes with dynamic stereogenic centers. Proc Natl Acad Sci USA 100:14623–14628
63. Chen HM, Parkinson JA, Parsons S, Coxall RA, Gould RO, Sadler PJ (2002) Organometallic ruthenium(II) diamine anticancer complexes: arene-nucleobase stacking and stereospecific hydrogen-bonding in guanine adducts. J Am Chem Soc 124: 3064–3082
64. Baik MH, Friesner RA, Lippard SJ (2003) Theoretical study of cisplatin binding to purine bases: why does cisplatin prefer guanine over adenine. J Am Chem Soc 125:14082–14092